JACS
JOURNAL OF THE AMERICAN CHEMICAL SOCIETY

COMMUNICATION

pubs.acs.org/JACS

Disproportionation of Dipyrrolylquinoxaline Radical Anions via the Internal Protons of the Pyrrole Moieties

Shunichi Fukuzumi,[*,†,‡] Kentaro Mase,[†] Kei Ohkubo,[†] Zhen Fu,[§] Elizabeth Karnas,[†,⊥] Jonathan L. Sessler,[*,⊥,#] and Karl M. Kadish[*,§]

[†]Department of Material and Life Science, Graduate School of Engineering, Osaka University, ALCA, Japan Science and Technology Agency, Suita, Osaka 565-0871, Japan

[‡]Department of Bioinspired Science, Ewha Womans University, Seoul 120-750, Korea

[⊥]Department of Chemistry & Biochemistry, The University of Texas, Austin, Texas 78712-0165, United States

[#]Department of Chemistry, Yonsei University, Seoul, 120-749, Korea

[§]Department of Chemistry, University of Houston, Houston, Texas 77204-5003, United States

Supporting Information

ABSTRACT: Disproportionation of dipyrrolylquinoxaline radical anions occurs via hydrogen atom transfer from the pyrrole moiety to the quinoxaline moiety to produce monodeprotonated dipyrrolylquinoxaline anions and monohydrodipyrrolylquinoxaline anions. In contrast, simple quinoxaline radical anions without pyrrole moieties are stable, and disproportionation occurs only in the presence of external protons.

Chart 1

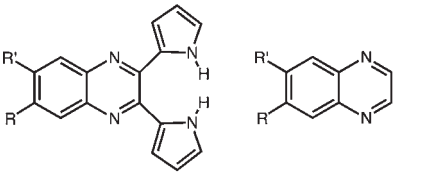

$1H_2$: R = NO_2, R' = NO_2
$2H_2$: R = H, R' = NO_2
$3H_2$: R = H, R' = H

4: R = NO_2, R' = NO_2
5: R = H, R' = NO_2
6: R = H, R' = H

Disproportionation of one-electron-reduced species plays an important role in converting one-electron processes to two-electron processes in a variety of chemical and biological redox reactions.[1,2] Notable examples are the disproportionation (dismutation) of superoxide anion and the disproportionation of semiquinone radical anions in photosynthesis.[3−5] In both cases, external protons are required for the disproportionation to occur.[6−8] Furthermore, to the best of our knowledge there are no examples in the literature, chemical or biological, where disproportionation of radical anions is mediated by internal protons, i.e., those present within the compounds that are reduced.

We report herein the first example of such a transformation. Specifically, we describe the preparation and chemical fate of dipyrrolylquinoxaline-derived radical anions and show that the internal pyrrole protons are involved in the disproportionation of these radical anions. The electron-transfer reduction of the dipyrrolylquinoxalines of this study is compared with that of the same quinoxaline units without pyrrole moieties, and, as detailed below, dramatic differences are seen. In particular, the radical anions of simple quinoxalines lacking appended pyrrole subunits are stable, with disproportionation occurring only in the presence of external protons.

In this study, the redox properties of the three dipyrrolylquinoxaline derivatives shown in Chart 1, namely, 2,3-dipyrrol-2′-yl-6,7-dinitroquinoxaline ($1H_2$), 2,3-dipyrrol-2′-yl-6-nitroquinoxaline ($2H_2$), and 2,3-dipyrrol-2′-ylquinoxaline ($3H_2$),[9,11] were examined. Also studied were the corresponding quinoxalines bearing the same number of electron-withdrawing nitro groups but without the two NH-containing pyrrole substituents (compounds **4**−**6**).

Figure 1 shows cyclic voltammograms of $1H_2$−$3H_2$ and **4**−**6** in acetonitrile (MeCN). In the case of $1H_2$ and $2H_2$, the first reduction is reversible when the negative potential scan is reversed just after the first cathodic peak (broken line in Figure 1). After the second and third cathodic peaks are observed, however, the corresponding anodic peak of the first reduction disappears (black line in Figure 1). In the case of **4** and **5**, which have the same quinoxaline units as $1H_2$ and $2H_2$ but lack the pyrrole moieties, the first and second reductions are both reversible and lead stepwise to formation of the corresponding radical anion and dianion. Only one reduction wave of **6** was observed without the electron-withdrawing NO_2 substituent. The differential pulse voltammetry (DPV) current of the first reduction of $1H_2$ is twice as large as the current for the second and third reductions, as shown in Figure S1 (see Supporting Information (SI)). The data from the DPV analysis of $1H_2$ are self-consistent with the cyclic voltammetry results and lead us to suggest that the first reduction is followed by a disproportionation of $1H_2^{\bullet-}$ to produce $1H^-$ and $1H_3^-$ (Scheme 1). The anion $1H^-$ is then further reduced in a series of stepwise one-electron transfers. Under these conditions, the DPV current for the first reduction of $1H_2$ is twice that measured for the reduction of $1H^-$ and $1H^{\bullet 2-}$ because $1H_3^-$ is not reduced.[10]

Received: January 30, 2011
Published: April 21, 2011

dx.doi.org/10.1021/ja200925e | J. Am. Chem. Soc. 2011, 133, 7284–7287

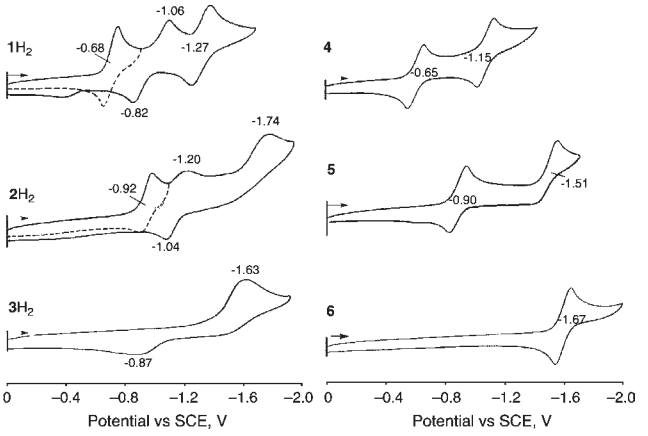

Figure 1. Cyclic voltammograms of $1H_2$−$3H_2$ and **4**−**6** in deaerated MeCN containing Bu_4NClO_4 (0.10 M) at 298 K. Scan rate, 0.1 V s^{-1}.

Scheme 1

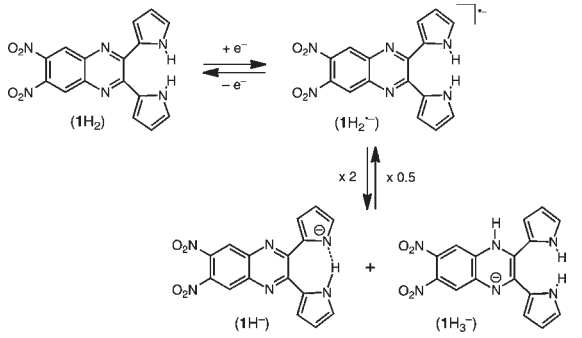

The reductions of $1H_2$ and $2H_2$ occur at more positive potentials than the reduction of $3H_2$, which lacks the electron-withdrawing NO_2 groups (Figure 1). In addition, the single observed reduction of $3H_2$ is irreversible under the same experimental conditions and also remains irreversible at rapid scan rates. Such a finding is consistent with the disproportionation of $3H_2^{\bullet-}$ being significantly faster than that of either $1H_2^{\bullet-}$ or $2H_2^{\bullet-}$.

In order to identify the processes that occur following the first reduction of $1H_2$, chemical reduction, involving electron transfer from cobaltocene ($CoCp_2$) to $1H_2$, was examined. The UV−vis spectral changes that occur during this reaction are shown in Figure 2a. Here, both the absorption changes at 325 and 553 nm were found to obey second-order kinetics, as illustrated in Figure 2b (for the second-order plot, cf. Figure S3). The kinetic isotope effect was determined to be 1.9 by using deuterated $1H_2$ ($1D_2$) (see Figure S4). This leads us to suggest that rapid electron transfer takes place from $CoCp_2$ to $1H_2$ to afford the radical anion $1H_2^{\bullet-}$ (λ_{max} = 325 nm) and $CoCp_2^+$ (λ_{max} = 260 nm), a process that is followed by the disproportionation of $1H_2^{\bullet-}$ via a hydrogen-atom transfer or a concerted proton-coupled electron-transfer (not stepwise) process, as shown in Scheme 1. The products of the disproportionation were examined by ^{1}H NMR spectroscopy and confirmed to be $1H^-$ and $1H_3^-$ (see Figures S5 and S6). The same monodeprotonated product ($1H^-$) could also be obtained by the reaction of $1H_2$ with tetrabutylammonium hydroxide (Bu_4NOH), as described in the literature;[12] this species is characterized by an absorption band at λ_{max} = 553 nm, as seen in Figure 2 and also in Figure S8.[13]

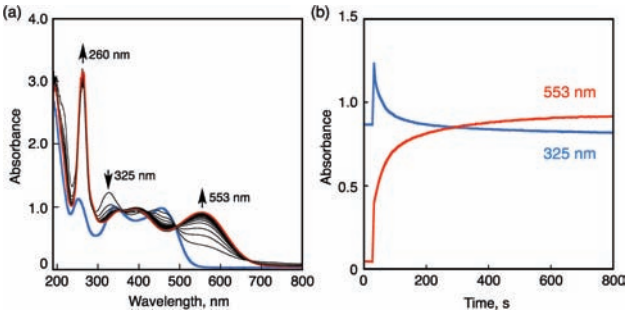

Figure 2. (a) Absorption spectral changes observed upon electron transfer from $CoCp_2$ (5.0×10^{-5} M) to $1H_2$ (5.0×10^{-5} M) in MeCN at 303 K. (b) Time courses for these changes recorded at 325 and 553 nm.

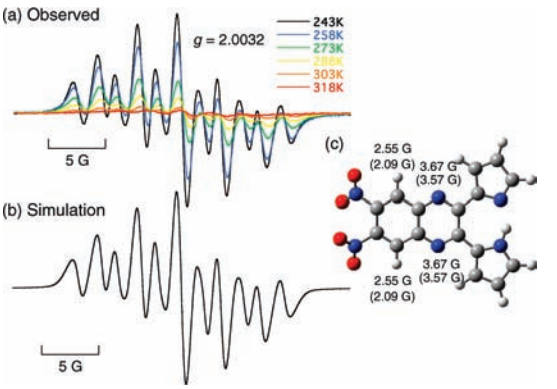

Figure 3. (a) EPR spectra of $1H_2^{\bullet-}$ produced via electron transfer from $CoCp_2$ (1.0 mM) to $1H_2$ (1.0 mM) in MeCN at various temperatures. (b) Simulated spectrum of $1H_2^{\bullet-}$ using hyperfine coupling constants (hfc) and those predicted by DFT. (c) DFT optimized structure of $1H_2^{\bullet-}$ with hfc values together with the calculated values given in parentheses.

Our assignment of a strong N−H−N hydrogen bond in the monodeprotonated product from $1H_2^{\bullet-}$ (Scheme 1) is based on the observation of ^{1}H NMR spectral features analogous to those seen previously for the same compound.[12] The anion $1H_3^-$ was also produced by the electron-transfer reduction of $1H_2$ with 2 equiv of $CoCp_2$ in the presence of 1 equiv of trifluoroacetic acid (Figure S6d).[14]

The disproportionation equilibrium of $1H_2^{\bullet-}$ was examined by measuring the electron paramagnetic resonance (EPR) spectrum of $1H_2^{\bullet-}$ produced by electron transfer from $CoCp_2$ to $1H_2$ at various temperatures (Figure 3a). The simulated hyperfine coupling constants of $1H_2^{\bullet-}$ agree well with the values estimated by DFT calculations (Figure 3b), providing support for spin delocalization on the quinoxaline moiety. Delocalization of spin on the quinoxaline moiety is also observed in the EPR spectrum of the related compound $4^{\bullet-}$ produced by electron transfer from $CoCp_2$ to **4** in MeCN (Figure 4). The radical anion $4^{\bullet-}$, a species that lacks the NH proton-containing pyrrole substituents present in $1H_2^{\bullet-}$, is stable and does not undergo disproportionation on the time scale of the experiment. However, the addition of external protons (in the form of trifluoroacetic acid) to a solution of $4^{\bullet-}$ in MeCN results in the rapid disappearance of the signals ascribed to $4^{\bullet-}$ as the result of facile disproportionation of $4H^{\bullet-}$ under these solution conditions (see Figure S9).

dx.doi.org/10.1021/ja200925e |*J. Am. Chem. Soc.* 2011, 133, 7284–7287

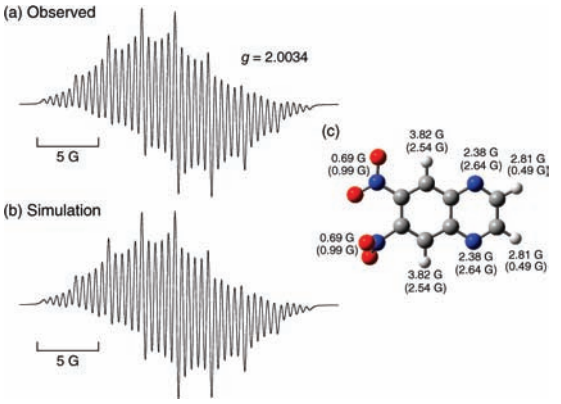

Figure 4. (a) EPR spectra of $\mathbf{4}^{\bullet-}$ produced via electron transfer from $CoCp_2$ (1.0 mM) to **4** (1.0 mM) in MeCN. (b) Simulated spectrum of $\mathbf{4}^{\bullet-}$ using hfc and those predicted by DFT. (c) DFT optimized structure of $\mathbf{4}^{\bullet-}$ with hfc values together with the calculated values given in parentheses.

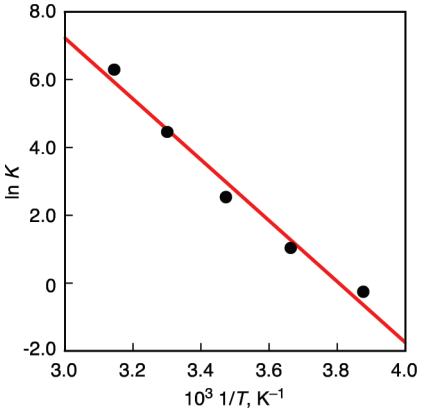

Figure 5. Van't Hoff plot of the disproportionation equilibrium constant (K) of $\mathbf{1H_2}^{\bullet-}$ as determined in MeCN.

The disproportionation equilibrium constant (K) for $\mathbf{1H_2}^{\bullet-}$ was determined using the observed concentration of $\mathbf{1H_2}^{\bullet-}$, a value that was determined by comparing the value of the double integration of the EPR signal with that of diphenylpicrylhydrazyl (DPPH), a stable radical reference (Table S1). A van't Hoff plot, shown in Figure 5, afforded ΔH and ΔS values of 18 kcal mol^{-1} and 68 cal mol^{-1} K^{-1}, respectively. The positive ΔH value obtained in this way indicates that the disproportionation of $\mathbf{1H_2}^{\bullet-}$ is endothermic.

The activation enthalpy ($\Delta H^{\ddagger}$) and entropy ($\Delta S^{\ddagger}$) were calculated to be 33 kcal mol^{-1} and −20 cal mol^{-1} K^{-1}, respectively, from the Eyring plot of the disproportionation rate constants determined from the second-order decay of $\mathbf{1H_2}^{\bullet-}$ at various temperatures (cf. Figure 6 and Table S2).

The disproportionation of $\mathbf{1H_2}^{\bullet-}$, $\mathbf{2H_2}^{\bullet-}$, and $\mathbf{3H_2}^{\bullet-}$ to produce monodeprotonated dipyrrolylquinoxaline anions ($\mathbf{1H}^{-}$, $\mathbf{2H}^{-}$, and $\mathbf{3H}^{-}$) and monohydrodipyrrolylquinoxaline anions ($\mathbf{1H_3}^{-}$, $\mathbf{2H_3}^{-}$, and $\mathbf{3H_3}^{-}$) was confirmed by spectroelectrochemical measurements as shown in Figure S10.[15] The absorption spectra of the monodeprotonated dipyrrolylquinoxalines ($\mathbf{2H}^{-}$ and $\mathbf{3H}^{-}$) produced by the reactions of $\mathbf{2H_2}$ and $\mathbf{3H_2}$ with Bu_4NOH, respectively, are shown in Figure S11 for comparison (the spectrum of $\mathbf{1H}^{-}$ is shown in Figure S8).

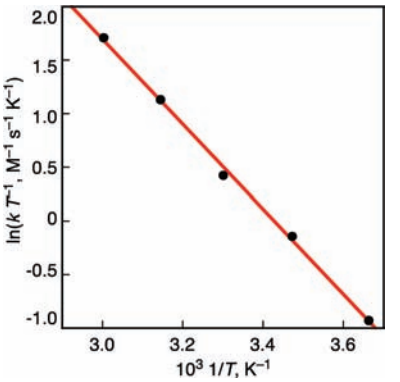

Figure 6. Eyring plot for the disproportionation of $\mathbf{1H_2}^{\bullet-}$ in MeCN.

In summary, the disproportionation of dipyrrolylquinoxaline radical anions produced by electron-transfer reduction of dipyrrolylquinoxaline occurs via hydrogen-atom transfer from the pyrrole moiety to the quinoxaline moiety. This gives the monodeprotonated dipyrrolylquinoxalines and monoprotonated dihydrodipyrrolylquinoxaline. In contrast, the same quinoxaline radical anions without the pyrrole moieties are stable in aprotic solvents. The present study furthers our understanding of disproportionation processes and provides a unique way to convert a one-electron reduction to a two-electron process without the need for external protons.

■ ASSOCIATED CONTENT

Supporting Information. Experimental details and spectroscopic data. This material is available free of charge via the Internet at http://pubs.acs.org.

■ AUTHOR INFORMATION

Corresponding Author

fukuzumi@chem.eng.osaka-u.ac.jp; sessler@mail.utexas.edu; kkadish@uh.edu

■ ACKNOWLEDGMENT

This work was supported by a Grant-in-Aid (No. 20108010 to S.F.) and a Global COE program, "the Global Education and Research Center for Bio-Environmental Chemistry", from the Ministry of Education, Culture, Sports, Science and Technology, Japan, and KOSEF/MEST through WCU projects (R31-2008-000-10010-0 and R32-2008-000-10217-0), Korea. Support from the U.S. NSF (grant CHE 0730053 to J.L.S.) and the Robert A. Welch Foundation (grants F-1018 and E-680 to J.L.S. and K.M. K., respectively) is gratefully acknowledged.

■ REFERENCES

(1) (a) Cukier, R. I.; Nocera, D. G. *Annu. Rev. Phys. Chem.* **1998**, *49*, 337. (b) Mayer, J. M. *Annu. Rev. Phys. Chem.* **2004**, *55*, 363. (c) Warren, J. J.; Tronic, T. A.; Mayer, J. M. *Chem. Rev.* **2010**, *110*, 6961.

(2) (a) Fukuzumi, S.; Fujioka, N.; Kotani, H.; Ohkubo, K.; Lee, Y.-M.; Nam, W. *J. Am. Chem. Soc.* **2009**, *131*, 17127. (b) Fukuzumi, S.; Kishi, T.; Kotani, H.; Lee, Y.-M.; Nam, W. *Nature Chem.* **2011**, *3*, 38. (c) Fukuzumi, S.; Kobayashi, T.; Suenobu, T. *Angew. Chem., Int. Ed.* **2011**, *50*, 728.

(3) Cabelli, D. E.; Riley, D.; Rodriguez, J. A.; Valentine, J. S.; Zhu, H. In *Biomimetic Oxidations Catalyzed by Transition Metal Complexes*; Meunier, B., Ed.; Imperial College Press: London, 2000.

(4) (a) Ellerby, L. M.; Cabelli, D. E.; Graden, J. A.; Valentine, J. S. *J. Am. Chem. Soc.* **1996**, *118*, 6556. (b) Okado-Matsumoto, A.; Fridovich, I. *J. Biol. Chem.* **2001**, *276*, 38388. (c) Smirnov, V. V.; Roth, J. P. *J. Am. Chem. Soc.* **2006**, *128*, 16424.

(5) (a) Aguilar-Martínez, M.; Macías-Ruvalcaba, N. A.; Bautista-Martínez, J. A.; Gómez, M.; González, F. J.; González, I. *Curr. Org. Chem.* **2004**, *8*, 1721. (b) Macías-Ruvalcaba, N. A.; Okumura, N.; Evans, D. H. *J. Phys. Chem. B* **2006**, *110*, 22043.

(6) Costeintin, C. *Chem. Rev.* **2008**, *108*, 2145.

(7) Disproportionation of radical anions is also facilitated by metal ions: (a) Jaworski, J. S.; Kosson, A.; Filipek, S.; Kolinski, M.; Kuck, D. *J. Phys. Chem. C* **2009**, *113*, 7436. (b) Yuasa, J.; Fukuzumi, S. *J. Am. Chem. Soc.* **2007**, *129*, 12912.

(8) Warren, J. J.; Mayer, J. M. *J. Am. Chem. Soc.* **2010**, *132*, 7784.

(9) Mizuno, T.; Wei, W.-H.; Eller, L. R.; Sessler, J. L. *J. Am. Chem. Soc.* **2002**, *124*, 1134.

(10) (a) Black, C. B.; Andrioletti, B.; Try, A. C.; Ruiperez, C.; Sessler, J. L. *J. Am. Chem. Soc.* **1999**, *121*, 10438. (b) Anzenbacher, P., Jr.; Try, A. C.; Miyaji, H.; Jursíková, K.; Lynch, V. M.; Marquez, M.; Sessler, J. L. *J. Am. Chem. Soc.* **2000**, *122*, 10268.

(11) The reaction scheme for electrochemical reduction of $\mathbf{1}H_2$ is shown in Scheme S1.

(12) Pietrzak, M.; Try, A. C.; Andrioletti, B.; Sessler, J. L.; Anzenbacher, P., Jr.; Limbach, H.-H. *Angew. Chem. Int. Ed.* **2008**, *47*, 1123.

(13) The titration of $\mathbf{1}H_2$ with Bu_4NOH indicates that $\mathbf{1}H^-$ and $\mathbf{1}^{2-}$ are formed by the reaction of $\mathbf{1}H_2$ with 1 and 2 equiv of Bu_4NOH, respectively (Figure S6).

(14) The structure of $\mathbf{1}H_3^-$ was estimated from DFT calculations (Figure S7). Protonation at the quinoxaline unit is more favorable rather than that at the nitro group based on a comparison of the energies of the $\mathbf{1}H_3^-$ isomers.

(15) The visible absorption spectra of the disproportionation products match those of monodeprotonated dipyrrolylquinoxaline anions ($\mathbf{1}H^-$, $\mathbf{2}H^-$, and $\mathbf{3}H^-$), because the monohydrodipyrrolylquinoxaline anions ($\mathbf{1}H_3^-$, $\mathbf{2}H_3^-$, and $\mathbf{3}H_3^-$) absorb only minimally in the visible region.